Safety Science 121 (2020) 394–402

Contents lists available at ScienceDirect

Safety Science

journal homepage: www.elsevier.com/locate/safety

Contact forces and dynamics of pedestrians evacuating a room: The column effect

Iker Zuriguel[a,*], Iñaki Echeverría[a], Diego Maza[a], Raúl C. Hidalgo[a], César Martín-Gómez[b], Angel Garcimartín[a]

[a] Departamento de Física y Matemática Aplicada, Facultad de Ciencias, Universidad de Navarra, Pamplona, Spain
[b] ETSAUN, Universidad de Navarra, Pamplona, Spain

ARTICLE INFO

Keywords:
Pedestrian dynamics
Evacuation
Contact pressure
Obstacle

ABSTRACT

We report experimental measurements obtained during the evacuation of 180 soldiers through a narrow door. Several conditions are analyzed in the evacuation drills, such as the degree of competitiveness (from rush to shove) and the influence of an obstacle placed before the exit. From the data, we compute the flow rate through the door and the velocity and density fields, as well as a map of the local evacuation time. We also present novel results on the pressure that the individuals exert on the wall adjacent to the door. Our study challenges the idea that an obstacle could be beneficial for pedestrian evacuations because of a hypothetical alleviation of pressure at the door. At the same time, we discover a correlation among the largest pressure peaks and the development of clogging.

1. Introduction

Since the publication of Helbing's pioneer work in 2000 (Helbing et al., 2000), it is believed that placing an obstacle in front of an exit could be beneficial for an evacuation, as it would increase the pedestrians flow rate. Indeed, there are several works in which this architectural solution has been experimentally tested (Helbing et al., 2005; Yanagisawa et al., 2009) revealing a positive but small effect that, given the intrinsic fluctuations of the bottleneck flow (Garcimartín et al., 2016; Nicolas et al., 2017), should be taken with care and reservation. Recent experiments (Shi et al., 2019) revealed that placing an obstacle leads to a weak flow rate improvement which was specially evident in moderately competitive evacuations through a door placed in the corner of a room. This last item is essential, as it was found that the placement of the exit at the corner had a stronger effect than the obstacle solution itself. It is not surprising that the extent to which the column affects the flow strongly depends on its position (Matsuoka et al., 2015; Frank and Dorso, 2011; Cristiani and Peri, 2017; Li et al., 2019; Lin et al., 2019): it would be detrimental if placed too close to the door, while it would have no effect at all if it is placed too far. The optimum position is expected to depend on the obstacle size and shape, two issues that also determine its effectiveness (Yano, 2018). These works (and many others dealing with the effect of columns in room evacuation) are nicely exposed in a recent review by Shiwakoti et al. (2019).

The reasons offered to explain this seemingly counterintuitive effect of the obstacle on the evacuation times are diverse and still under discussion (Jiang et al., 2014; Feliciani and Nishinari, 2018). Nevertheless, the most widely accepted hypothesis (Helbing et al., 2005) holds that the obstacle creates an emptiness in a region behind it, namely, downstream; hence facilitating conflict solving among people vying for space at the very door. If this were the case, placing a column would also be beneficial in terms of reducing the pressure felt by pedestrians approaching the door, which in some extreme instances could reach very high levels, leading to casualties. Unfortunately, experimental pressure measurements in evacuation drills are rather scarce. In a recent qualitative estimation (Pastor et al., 2015) a correlation was found between the force measured at the doorjamb and the competitiveness level. Pressure measurements have also been performed in experiments involving the flow of animals through a small gate (Wu et al., 2018), a scenario in which the flow rate improvement by the presence of a column has also been experimentally demonstrated (see (Zuriguel et al., 2016) for an example with sheep and (Wang et al., 2018) for mice).

Leaving aside the effect of placing an obstacle before the exit, it is important to remark the shortage of controlled evacuation experiments in which the physical pressure among pedestrians is significantly high. The few existing ones have provided highly valuable knowledge that

* Corresponding author.
E-mail address: iker@unav.es (I. Zuriguel).

https://doi.org/10.1016/j.ssci.2019.09.014
Received 27 May 2019; Received in revised form 27 August 2019; Accepted 12 September 2019

helped to clarify the physical reason behind the 'Faster is Slower' (FIS) effect (Pastor et al., 2015; Garcimartín et al., 2014; Haghani et al., 2019): it seems that the flow reduction only happens when people push each other in their way out of a room, hence suggesting that evacuation delays are not due to an increase of the people's desired velocity, but to the heightened pressure causing clogging at the door. Some of these works have also revealed the spontaneous emergence of undesired crowd movements in a direction perpendicular to the exit (Garcimartín et al., 2017) that resemble the ones reported in larger precincts (Bottinelli et al., 2016) and are sometimes described in terms of pedestrian turbulent motion (Helbing et al., 2007; Yu and Johansson, 2007; Moussaïd et al., 2011).

In a recent work, we experimentally investigated the obstacle role for highly competitive pedestrian evacuations, challenging the idea of its beneficial effect in terms of evacuation times (Garcimartín et al., 2018). To this end, several series of tests were performed in a range of conditions –for instance, with different crowd sizes, obstacle positions, and level of competitiveness–, all of which systematically lead to the same result: increasing the competitiveness (allowing people to push each other) reduces the flow rate, but placing the obstacle does not cause a noticeable effect at all (neither beneficial, nor detrimental). Interestingly, by a careful analysis of the third series of these experiments (with 180 soldiers in highly competitive conditions), it was discovered that placing a column screens the undesired pedestrian movements in the transversal direction that emerged in absence of the obstacle. This finding, which has not been reported before in bottleneck experiments or simulations, could be of practical importance in terms of preventing people falls. Nevertheless, in this previous work, some of the standard magnitudes measured in pedestrian dynamics (such as density and velocity field maps) were not reported.

In this work, we extend our previous analysis and present the spatial dependence of these magnitudes (and others such as the evacuation time). More importantly, we introduce pioneering data of the pressure measured at the door and near it. The time series of the contact force done by the crowd to both, the doorjamb and the wall adjacent to the door, is a new piece of information that gives a more meaningful picture of the evacuation dynamics.

2. Procedures

2.1. Evacuation drills

The evacuation drills involved 180 soldiers in the América 66 regiment of the Spanish army, and took place in an indoor gym at their barracks in Aizoáin (Navarra, Spain). Participation in the drills was voluntary, and as the soldiers could opt out at any time, their number in each evacuation is a little bit different (it ranges from 181 to 165). There were seven management staff, as well as several officers (some of whom participated in the evacuations), to ensure that no substantial risk was being taken. The 75 cm wide door was specially designed with a reinforced structure. In some of the evacuations, an obstacle was placed in front of the exit. It was a 1 m diameter cylindrical resin container filled with about one ton of water, a design that has two important advantages: i) the resin is extremely resistent and smooth, hence preventing injuries or brushes to the volunteers; ii) when emptied the obstacle was quite light, so it was easy to move allowing us to place it in the appropriate position, on top a rubber sheet to prevent sliding. When filled, the obstacle was heavy enough to avoid being displaced, something that cannot be taken for granted, as we learnt from previous experiments in which we used a 300 kg obstacle that was moved by a group of 80 persons (Garcimartín et al., 2018).

In all the evacuations the soldiers were asked to exit the room as soon as possible. In some cases they were allowed to moderately push each other as they found their way out (this scenario is called 'high competitiveness', **HC**); in other cases, only unintended, sporadic contacts were allowed (this scenario is called 'low competitiveness', **LC**). The other condition that was investigated during the evacuation drills was the presence of an obstacle. Several positions of the obstacle were tested, but it was always placed in front of the exit, aligned with the door center. The distance between the obstacle and the door was measured from the door to the closest point of the obstacle. In particular, we performed (a) 3 evacuations at low competitiveness without obstacle (NO/LC); (b) 3 evacuations at low competitiveness, with an obstacle placed 60 cm from the door (O60/LC); (c) 7 evacuations at high competitiveness without obstacle (NO/HC); (d) 6 evacuations at high competitiveness with an obstacle at 70 cm (O70/HC); (e) 6 evacuations at high competitiveness with an obstacle at 60 cm (O60/HC); and (f) 6 evacuations at high competitiveness with an obstacle at 50 cm (O50/HC).

The drills began with the participants gathering inside a rectangle painted on the floor of about 10×5 meters, so that the initial density was close to four persons per square meter. The door was centered at one of the long sides of the rectangle. A sound signal marked the beginning of the evacuation drill, and it was agreed that anybody could request a halt if any accident were to happen (such as a person falling to the floor); several staff, placed at different points, were ready to issue another sound signal in that case. After a blank drill, we performed the evacuations listed above with some small pauses in between. No serious incident was reported.

2.2. Tracking and data processing

In order to characterize the pedestrian dynamics, we recorded the evacuation drills with two zenithal cameras (one inside the gym and one outside). The camera outside the room was a standard video camera (704×576 pixels) and allowed us to detect the exit times of each pedestrian. From these data the flow rates or the heading times of consecutive individuals were calculated as reported in Garcimartín et al. (2018). The camera inside the gym was a 4 K camera (3840×2160 pixels) recording at 25 frames per second. It was placed at a height of 8 m, reaching a field of view of 6×3.2 m. The system was calibrated so that primary aberrations were corrected to within 2%. In order to track the individuals, we provided a red hat to every person. An image processing software written by us (Garcimartín et al., 2017) was used to track the soldiers trajectories. Thus, the particle tracking measurements provided the location of individuals along time $\mathbf{r}_i(t)$, where i denotes a given person. From them, it is easy to obtain the velocity of individuals as $\mathbf{v}_i(\mathbf{r}_i, t) = \Delta\mathbf{r}_i/\Delta t$. The value of Δt must be large enough to include more than one step, otherwise the sideways velocity resulting from the asymmetry of single steps would appear prominently. Aiming to filter out these oscillations, we have taken $\Delta t = 1.6$ seconds, a value that corresponds to an exact number of video frames. Moreover, as the position of individuals changes very little from frame to frame, calculating the velocity for every single frame is not practical. We have decided to obtain a value for the velocity every 12 frames (*i. e.* every 0.48 s), because this is about the time it takes for an individual to move a distance approximately equal to its own size. In this way, we have a discrete set of velocities $\{\mathbf{v}_i(\mathbf{r}_i, t)\}$ for each evacuation.

From the pedestrian data we have calculated macroscopic fields, such as the density and velocity fields, as well as the spatial dependence of the evacuation time. In order to obtain a continuous field for the density, we have implemented the coarse-graining method introduced by Goldhirsch (2010). It amounts to spreading uniformly the mass of a person m over a circle (other shapes could also be considered). The space is then discretized in a grid, and the macroscopic density field $\rho(\mathbf{r}, t)$ is calculated by adding all the masses at each square of the grid and normalizing with respect to m. Mathematically, this amounts to a convolution of a boxcar function $\phi(\mathbf{r})$ (in two dimensions, it has a disk shape) with the locations $\mathbf{r}_i(t)$. We have taken the diameter of the disk equal to the average distance between the shoulders of a person (which is about 45 cm). Bigger sizes can be taken, which would smooth the density field; also, other functional forms can be used, such as a

Gaussian instead of a boxcar function. We have taken a straightforward approach and opted for the simplest method (a flat disk of 45 cm diameter). Normalization requires that $\int_A \phi(\mathbf{r} - \mathbf{r}_i(t))d\mathbf{r} = 1$, so the height of the disk is $1/S$, where S is the surface of the disk. Note that ϕ has dimensions of the inverse of an area. We have taken $m = 1$, which amounts to consider all the persons identical.

With these definitions we can write

$$\rho(\mathbf{r}, t) = \sum_i m\,\phi(\mathbf{r} - \mathbf{r}_i(t))$$

where ρ has units of persons per unit surface.

We then performed two averages: one over time, and another for the ensemble of evacuations performed under a given condition. The time average $\bar{\rho}(\mathbf{r})$ is done by taking all times t of a given evacuation between the exit of the 20^{th} and the 110^{th} individuals. This is done because we have observed a transient when people begin the evacuation that lasts until the 12^{th} individual (more or less) has evacuated the room. During this short period of time all pedestrians move towards the door, leading to a dramatic growth of density: from the initial (4 pedestrians per square meter) to more than 8. Also, the last part of the evacuation is removed from the analysis. This is done as we realized that the last pedestrians were not really behaving in a highly competitive manner as their colleagues did. Also, when only a few people remain in the room, some of the regions analyzed were empty so it does not make sense to calculate the density there. In this way we are confident that the situation between the exit of the 20^{th} and the 110^{th} individuals is approximately the same in the camera field of view. After this we performed an ensemble average, taking the mean $\langle\bar{\rho}(\mathbf{r})\rangle$ of all the densities $\bar{\rho}(\mathbf{r})$ corresponding to a given set of evacuations.

For the velocity, the coarse graining procedure is performed in a similar way, for each one of the velocity components $\mathbf{v} = (v_x, v_y)$. We first calculate the momentum density $\mathbf{p}(\mathbf{r}, t)$, which is the convolution of $m\mathbf{v}$ with ϕ, taking $m = 1$, and then we divide it by the density $\rho(\mathbf{r}, t)$. We finally obtain $\langle v_x\rangle$ and $\langle v_y\rangle$, from which we can calculate $\langle v\rangle = \sqrt{\langle v_x\rangle^2 + \langle v_y\rangle^2}$ (the subscript i has been dropped for the sake of clarity). Let us remark that the particular choice for the parameters (such as the disk diameter, the time interval and so on) have little effect on the final result if the numbers are changed by a factor of two, say. Also, as we noticed that people far from the door sometimes hesitate about their way out, we only calculate $\langle v\rangle$ for positions closer than 3 m from the door.

We have also calculated the evacuation time spatial distribution, which is a representation of the average time the pedestrians need to reach the exit from a particular location $\mathbf{r}$. In this case, we have considered that the most sensible procedure is to measure this time for every single person in the camera field of view at 10 s intervals. In this way, we are sure that we are considering a different spatial configuration of persons in each measurement. For the reason pointed above, and because farther from there we have less data, we only calculated exit times for positions closer than 2.5 m from the door. We began after the 12^{th} individual has left the room and we finished when there are less than 20 people in the room. Then we obtained the time taken by each pedestrian to reach the door from the positions of the persons in each one of the selected frames. In this way, we have collected exit times for at least one thousand locations for every experimental condition. We then fitted an interpolated surface using a triangulation-based natural neighbor interpolation.

2.3. Pressure measurements

We recorded contact pressure measurements by means of a pressure mapping sensor placed at the left side of the door. The sensor was covered with black self-adhesive vinyl as shown in Fig. 1. The same lining was also glued at the right side of the door in order to keep the same conditions at both sides. The pressure mapping sensor is a Teskscan model 5400 N-A, consisting of a 1768 sensors in all, arranged into 52 rows and 34 columns, covering a total area of 88.4 cm height × 57.8 cm width. The mesh location on the door is represented in Fig. 1, with the lowest row of sensors at a height of 82 cm. As the sensor array is pliable, we bent it around the doorjamb: the first 5 columns were on the door jamb while the rest (29) were on the wall.

The size of each sensor was 1.7 × 1.7 cm and the output signal was digitized in 256 levels. The scale factor, that allows to convert these units into pressure, depends on the sensitivity of the instrument –that can be tuned within a certain range– and was determined by a calibration before the experiment. The calibration is crucial to avoid sensor saturation; we selected the sensitivity so that less than one in 10000 measurements reached a level higher than 250.

We proceeded by synchronizing the pressure measurements with the video recordings. We have taken the passage of the first pedestrian as the initial time. As the evacuation total time differs slightly from one drill to another, we only consider pressure values obtained until the shortest total evacuation time for each experimental condition. We also noticed that the pressure at the doorjamb was much higher than the pressure on the wall, and we have therefore analyzed the two regions separately, *i. e.* we saved the first 5 columns of sensors corresponding to the door jamb in a file, and then the other 29 columns, corresponding to the wall, in a different one.

3. Pedestrian dynamics

In the evacuation drills reported here, it was already shown that the flow rate J (in units of persons per second) through the 75 cm wide door was lower when there was competitiveness among the pedestrians. Also, it was reported that the presence of an obstacle did not improve J: on the contrary, it could even be slightly reduced if the obstacle was placed too close to the door (Garcimartín et al., 2018). As a summary, in Table 1 we show the average flow rates for each experimental condition analyzed in this work.

3.1. Density and velocity fields

Let us first consider the density and velocity fields (Fig. 2) in the different scenarios, investigated by the procedure outlined in Section 2. As noted, in the evacuations without obstacle the density maps display different patterns for high and low competitiveness. For the first condition, one can see a semicircular region of high density, while for the second one the regions near the wall have a relatively low density. The confirmation of this feature, which was already reported in evacuations with a reduced number of pedestrians (Garcimartín et al., 2017), suggests that the cylindrical symmetry in the density fields could be taken as a hallmark of very competitive behavior during the evacuation. Also, we would like to stress that the density in the high competitive scenario (Fig. 2b) reaches peak values in the range of 10 persons per square meter. These values are higher than the ones reached in previous evacuation drills, carried out by students, where the highest densities reached up to about 9 persons per square meter. This highlights the substantial degree of confinement achieved in present experiments, which can be caused either by a more aggressive behavior of the individuals or by the higher number of participants in the drills. When the obstacle is present (Fig. 2c, d, e, f) people avoids the region behind it, a feature reflected by notably lower values of the density in this region. On the contrary, the densities around the obstacle in zones closer to the door are remarkably high. This effect is observed independently on the competitiveness degree although, as expected, the density values observed for the competitive scenario are considerably higher.

The velocity fields obtained (right column of Fig. 2) are in good agreement with the density outcomes. When there is no obstacle, the speed for the LC case shows approximately azimuthal symmetry. As can be seen, far from the door and the wall, the speed is rather constant for any given fixed distance to the door center, r, and so the contour lines of $\langle v\rangle$ are not far from a azimuthal symmetry. These profiles get rather

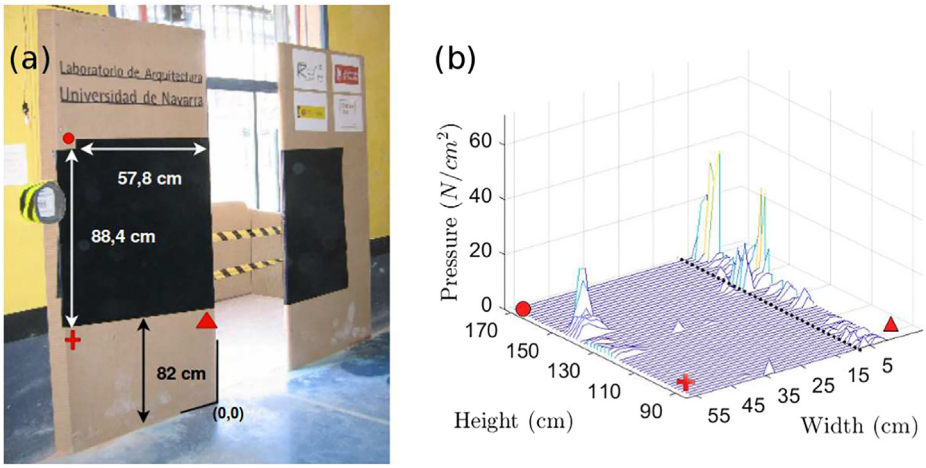

Fig. 1. A) Photograph of the door with the dynamic pressure mapping system (*covered with black lining, at left*). B) Example of an instantaneous pressure field registered during a competitive evacuation without obstacle. The dashed line separates the two regions (doorjamb and wall) where pressure has been analysed. The symbols in both plots are used to mark three spatial references.

Table 1
Average flow rate, in persons per second, for the different evacuating conditions. Error is given as 95% confidence intervals. HC and LC stand for high and low competitiveness. NO: no obstacle; O*nn* means the obstacle is placed at *nn* cm from the door.

Obstacle	Competitiveness	Flow rate (*persons*/s)
NO	LC	2.9 ± 0.1
NO	HC	2.5 ± 0.1
O50	HC	2.2 ± 0.1
O60	LC	2.7 ± 0.1
O60	HC	2.3 ± 0.1
O70	HC	2.4 ± 0.1

warped as competitiveness increases, and higher speeds are only found just in front of the door. This implies that, whereas in a non competitive scenario the only important magnitude defining the velocity is the distance to the door, in competitive conditions, approaching the door head-on favours higher velocities, and positions near the wall lead to lower velocities. This is in agreement with previous results (Garcimartín et al., 2017).

3.2. Evacuation time

Let us now investigate the spatial dependence of the evacuation time, as measured by the time it would take for a pedestrian to reach the exit from a given position in the room. Our aim is to find out whether or not there are particular places from where evacuation is easier or more difficult. The spatial representation of the evacuation times is shown in Fig. 3, left column.

In the central column of Fig. 3 we represent the evacuation time rescaled by r^2 (r being the distance to the door). The reason for this scaling is the following. It is obvious that the farther a pedestrian is from the door, the longer it will take to reach it. It makes sense therefore to consider the time taken to reach the door per unit length. Moreover, if the flow rate and the density are constant, because of the continuity condition, the speed should be proportional to $1/r$. Then the evacuation time should be divided again by r, leading to a rescaling with r^{-2}. Another way to understand this rescaling is to consider that the number of people closer to the door than a given individual at a distance r to the door is proportional to the area $\pi r^2/2$, so if the flow and density are constant the exit time will be proportional to r^2. A check for this argument is the homogeneous map of the rescaled evacuation time observed for the non competitive case without obstacle (Fig. 3, *g*). In this scenario, the evacuation time from a given place only depends on the distance to the door.

We also examined the rescaled evacuation time averaged in uniformly spaced angle intervals. The third column of Fig. 3 displays these angle histograms. This provides a visual assessment to the angular symmetry of the evacuation times, so it is straightforward to discern whether there is any direction from which it is easier to reach the door. As shown in Fig. 3m, the histogram is quite uniform for the NO/LC case. This behavior is attributed to a scenario where pedestrians generally cooperate giving way to their neighbours, hence leading to a smooth evacuation.

For high competitiveness (Fig. 3b), the first conspicuous result is an overall increase of the evacuation times. In addition, it is interesting to note that the maps loose the cylindrical symmetry. Courses heading perpendicularly to the door boast lower evacuation times than those directions approaching from the sides, corresponding to pedestrians moving along the wall, which end up being the worst positions for reaching the door quickly. This can be seen distinctly in the angular histograms of the rescaled evacuation times (Fig. 3n). When the obstacle is placed in front of the door for the competitive case (Fig. 3c, e, f), the situation improves for those people near the wall, although the times are still slightly larger than in the non-competitive case. Nevertheless, the region behind the obstacle becomes clearly worsened. The courses with the lowest evacuation times are those in between the wall and the obstacle, as it becomes readily evident from the angular histograms of rescaled times (Fig. 3o, q, r). A similar effect (but, of course, less marked as the evacuation is quicker overall) is observed for the non competitive case with an obstacle (Fig. 3d, j, p). These results are congruent with the velocity fields, as displayed in Figs. 2. In particular, the cylindrical symmetry is only observed in the case of low competitiveness, without an obstacle. For a competitive situation, the shortest evacuation time corresponds to positions in front of the exit (90 degrees), which is consistent with the higher velocities observed in this region. When the obstacle is placed in front of the door, the maps are dramatically altered and the longest evacuation times are found for the region behind the obstacle. Interestingly, for competitive conditions, the low velocities in the lateral regions (near the walls) do not disappear completely. This is evidenced by the red spots in the bottom corners of Figs. 2i, k, l, and the higher values of the angle histograms shown in Fig. 3o, q, r, for angles close to 0 and 180.

4. Pressure at the doorjamb and adjacent wall

Let us first display the temporal evolution of the pressure in four representative scenarios: NO/LC, NO/HC, O50/HC, and O70/HC (Fig. 4). To this end, and as a first approximation, we have calculated the average pressure over all sensors along time in each one of the two regions mentioned above: wall and doorjamb. The temporal series for each single evacuation drill is shown with a gray line, and the ensemble average (for all the evacuations performed under the same conditions) with a red line. Several pieces of information can already be gathered

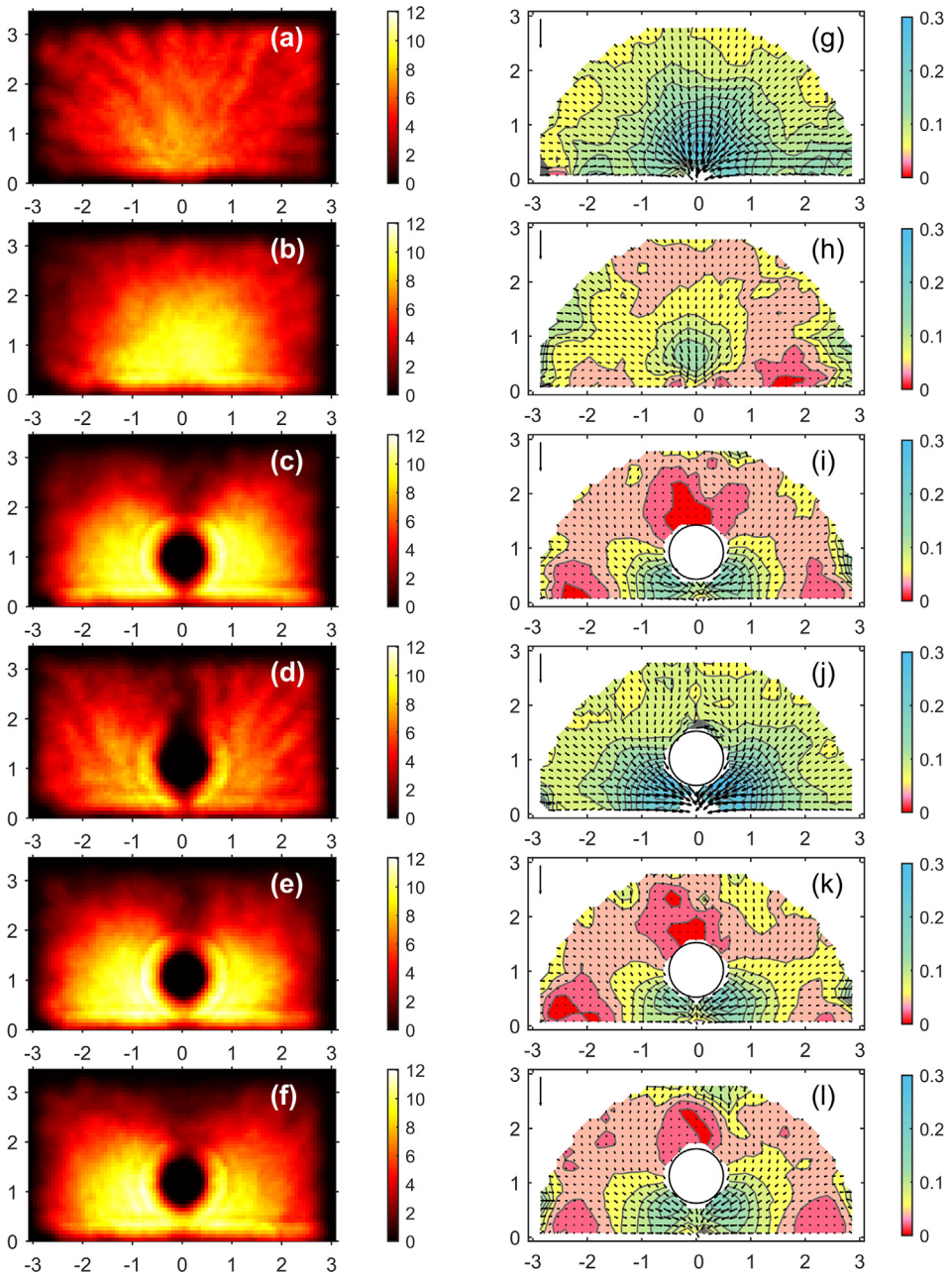

Fig. 2. Density and velocity maps for the six different scenarios explored. In the left column, density fields for (a) NO/LC, (b) NO/HC, (c) O50/HC, (d) O60/LC, (e) O60/HC, (f) O70/HC. The colour scale at the right (which is the same in all cases) indicates the average local density in $persons/m^2$. The spatial units in vertical and horizontal direction are meters. In the right column, velocity fields for (g) NO/LC, (h) NO/HC, (i) O50/HC, (j) O50/LC, (k) O60/HC, (l) O70/HC. The colour scale at the right (which is the same in all cases) indicates the average local velocity modulus in m/s. The scale at the left top corner is $0.5m/s$. The spatial units in vertical and horizontal direction are meters. (For interpretation of the references to colour in this figure legend, the reader is referred to the web version of this article.)

from the plots of Fig. 4. First, remark the highly fluctuating nature of the pressure values. This feature underlines the need to perform several evacuation drills under the same conditions in order to average out the noise and to avoid putting forward potentially misleading conclusions. Second, note how the pressure level for non competitive scenarios is much lower than in high competitive ones. Third, it can be seen that the pressure at the doorjamb is much higher (by about one order of magnitude) than on the wall.

Surprisingly, the pressure measurements at the wall in HC conditions do not reveal significant differences if an obstacle is present or not (compare Fig. 4b, c, d). In all these cases, there is a sudden growth of pressure at the beginning of the drill, and then a slow decrease that probably has to do with the reduction of people in the room. On the contrary, the measurements at the doorjamb (bottom row in Fig. 4) differ markedly depending on the presence and position of the obstacle. Indeed, the obstacle presence reduces the pressure in the case of high competitiveness (compare Fig. 4f, g, h), an effect that seems more marked when the obstacle is closer to the door. In addition, note how the reduction of pressure with time that was observed in the wall measurements is not that evident at the doorjamb; only maybe in the NO/HC case (Fig. 4f).

A problem with the representation in Fig. 4 is that the average pressure calculated at every single time does not properly reflect the spatial inhomogeneity of the pressure measurements (see for example Fig. 1b). Indeed, the figures were obtained after averaging over a region where most of the sensors do not detect any pressure at all, so it is

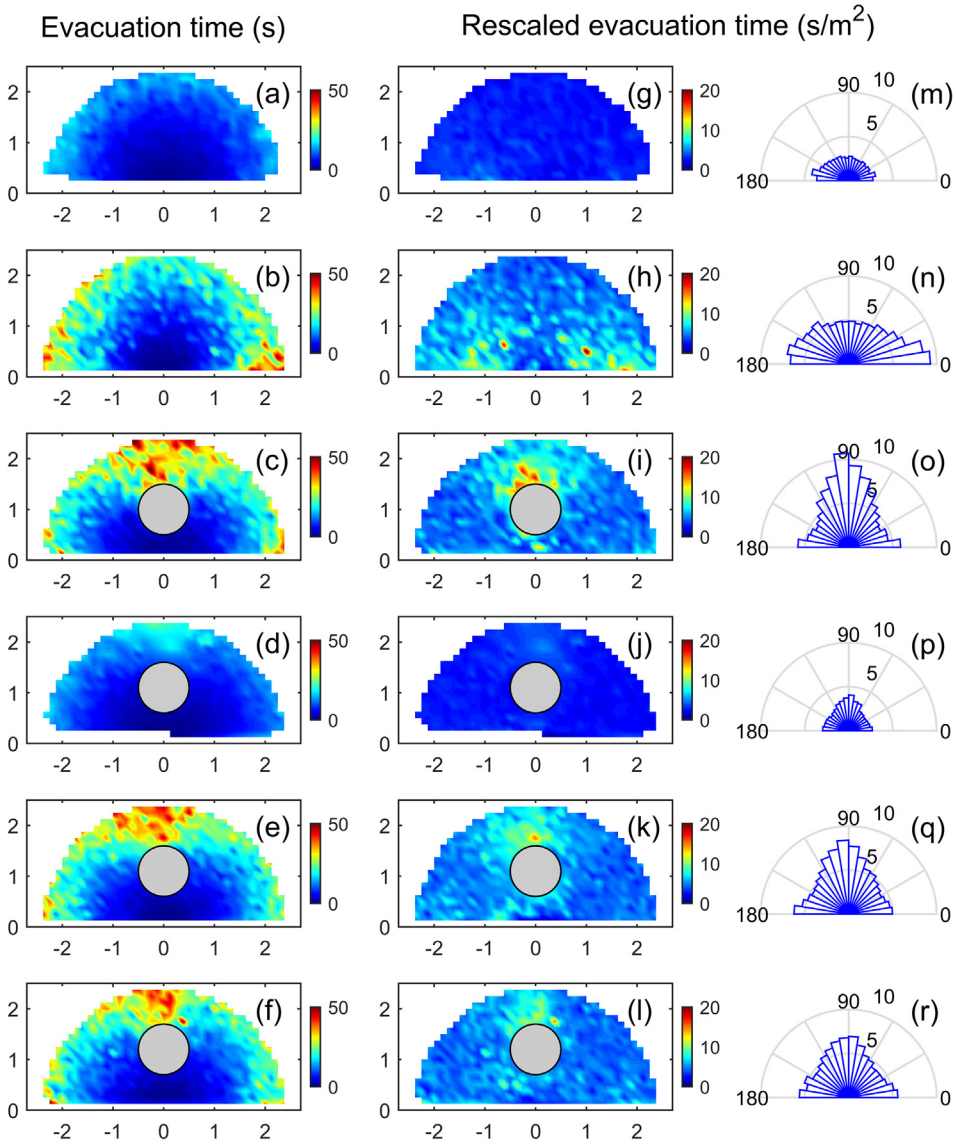

Fig. 3. Spatial dependence of the evacuation time for the different scenarios explored. The time it takes to reach the door is displayed in the first column for (a) NO/LC, (b) NO/HC, (c) O50/HC, (d) O60/LC, (e) O60/HC, and (f) O70/HC. In the second column, the evacuation time divided by r^2 is shown for (g) NO/LC, (h) NO/HC, (i) O50/HC, (j) O50/LC, (k) O60/HC, and (l) O70/HC. In both columns, colour scales at the right indicate the evacuation time or rescaled evacuation time. The spatial units in vertical and horizontal direction are meters; the door center is located at (0,0). In the third column, the angle histogram of the rescaled evacuation times for (m) NO/LC, (n) NO/HC, (o) O50/HC, (p) O50/LC, (q) O60/HC, and (r) O70/HC. Angles 0 and 180 correspond to pedestrians standing near the wall, and 90 to a direction perpendicular to the door. Radial units (*gray semicircles*) are s/m^2.

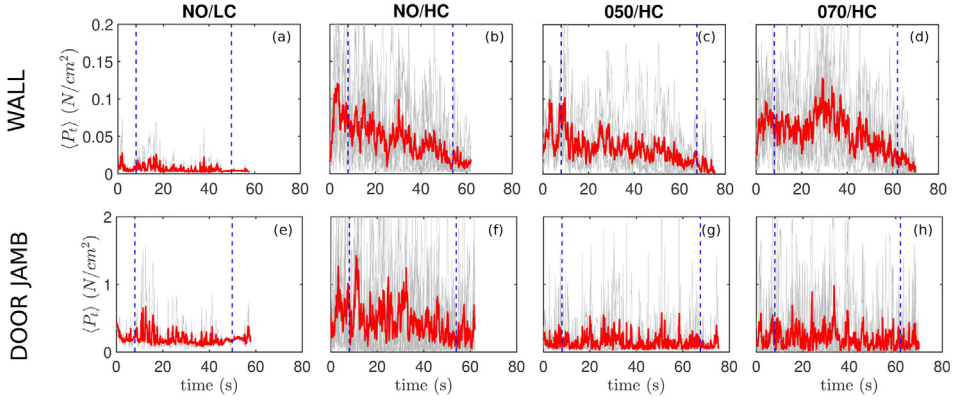

Fig. 4. The time series of the average pressure in four different experimental conditions, as indicated on top. The pressure value at a given time is the average of all the sensor units in the two regions analyzed: the door jamb (*bottom row*) and the wall (*top row*). Grey lines correspond to each evacuation drill; the red line is the ensemble average of all drills performed under the same conditions. (For interpretation of the references to colour in this figure legend, the reader is referred to the web version of this article.)

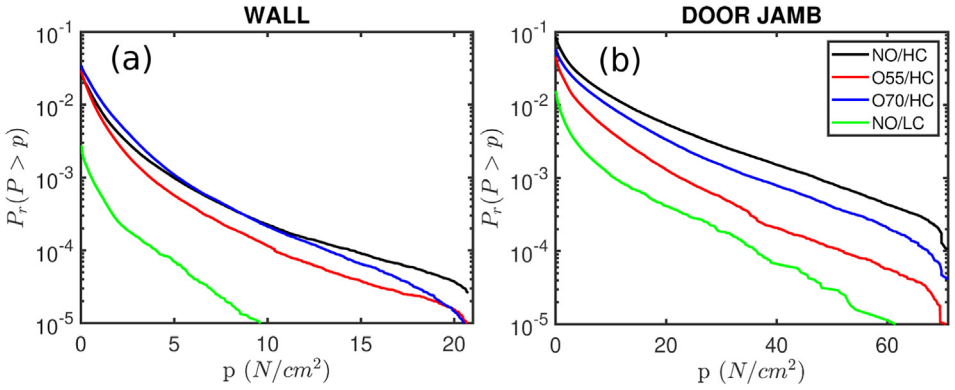

Fig. 5. Survival functions of the pressure measurements of all the sensors over the time interval from 10 to 50 s after the beginning of the evacuation, and for all the drills performed under the same conditions. Four different scenarios are represented with the colors indicated in the legend. (a) Wall measurements. (b) Doorjamb measurements.

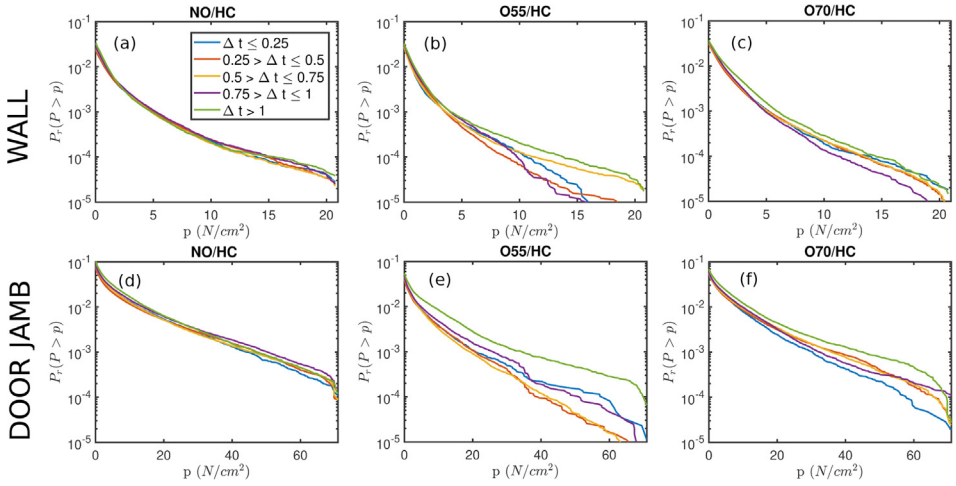

Fig. 6. Survival functions of the pressure measurements taken at different flowing conditions for three evacuation scenarios (all of them competitive) as indicated at the top of each panel. In the top row, pressure measurements at the room wall; at the bottom, pressure measurements at the doorjamb.

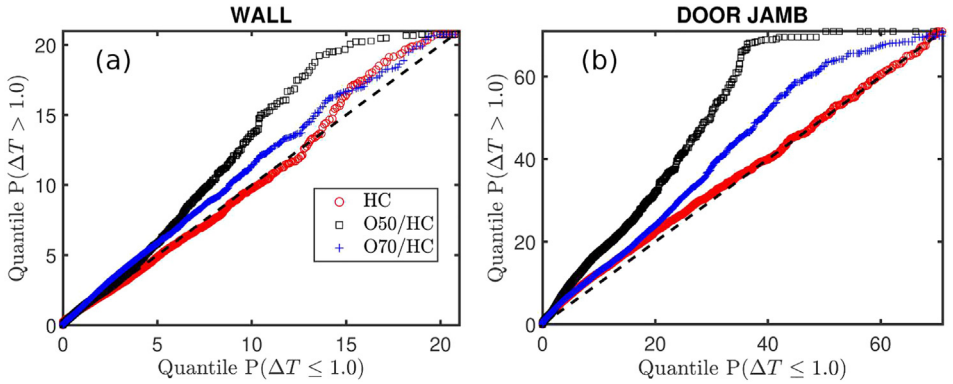

Fig. 7. Q-Q plot of the pressure distributions corresponding to $\Delta t \leqslant 1$ and $\Delta t > 1$. Results for the pressure at (a) the wall, and (b) the doorjamb are shown for the three experimental conditions indicated in the legend.

doubtful whether they are meaningful if one wants to describe the pressure that an individual is locally applying to the door. The problem worsens if we take into account that the harmful effects of pressure in humans are mainly related to their peak values. For this reason, and in order to get some insight about the local pressures, we represented the survival function of the values of all sensors in the matrix (Fig. 5). The curves were obtained by taking all the pressure values registered during all the evacuations made under the same conditions, for times ranging from 10 s to 50 after the beginning of the drill (this is done to avoid the influence of initial and final transients). As explained before, we analyzed separately the pressure at the doorjamb and the pressure at the wall. The survival functions obtained confirm several of the findings revealed by the temporal evolutions: in all cases, the pressure magnitude for low competitiveness is much lower than in high competitiveness; the pressure values at the doorjamb are higher than at the wall; the presence of the obstacle has not a net effect in the pressure registered at the wall (although it seems that when the obstacle is at 50 cm, a small reduction of pressure takes place); the pressure at the doorjamb is notably affected by the presence of the obstacle; and the closer the obstacle is to the door, the lower the pressure at the doorjamb is. In addition to these issues, the survival functions allow to get a more accurate picture concerning the magnitude that the maximum local pressure may reach in each condition.

Finally, with the aim of understanding why the obstacle does not

have any noticeable effect on the evacuation time, we have looked into the relationship between the clogging times –namely, the time lapses during which nobody goes through he door– and pressure. To this end, we obtained the passage time of each individual through the door, and then we calculated the clogging time Δt as the time interval until the exit of the next person; an obstruction at the door corresponds to high values of Δt. Next, we calculate the survival functions of the pressure measurements but grouping them according to the Δt value corresponding to the moment at which the pressure was taken. If the pressure is larger when the door is blocked, the survival functions obtained for high Δt would exhibit higher pressures. Otherwise, if high pressure values are caused by pedestrians haphazardly bumping against the door, and if these collisions are harder and more frequent when people flow more fluently, then the survival functions obtained for low Δt would reflect higher values.

In Fig. 6 we represent the survival functions of the pressure measurements at both, the doorjamb and the wall, for three cases: NO/HC, O50/HC and 070/HC. In each situation, we have classified the flowing conditions according to these five criteria: (i) $\Delta t \leqslant 0.25$; (ii) $0.25 < \Delta t \leqslant 0.5$; (iii) $0.5 < \Delta t \leqslant 0.75$; (iv) $0.75 < \Delta t \leqslant 1$; and (v) $\Delta t > 1$ seconds. Surprisingly, for the case in which there is no obstacle, the pressure recordings do not show any perceptible dependence on the flowing condition (neither at the room wall nor at the doorjamb). On the contrary, when there is an obstacle, the tails of the survival functions of the pressure at the doorjamb for $\Delta t > 1$ are systematically higher than the others. This indicates an increment of the pressure at the doorjamb when the flow is arrested, a feature that becomes more obvious if the obstacle is near the door (O50/HC, Fig. 6e) than if it is placed farther (O70/HC, Fig. 6f). A similar behavior can be noticed in the wall measurements for the case O50/HC (Fig. 6b) where the probability of finding higher pressures is also larger for $\Delta t > 1$. From these results we can conclude that the development of high pressures (specially at the doorjamb) is linked to the formation of clogs at the door; yet for some reason this correlation only appears when the obstacle is present.

In order to confirm this finding, we have split all the pressure measurements in just two sets: one that corresponds to clogs longer than one second ($\Delta t > 1$), and another for all the other cases ($\Delta t \leqslant 1$). Then, from the two distributions of pressure, we have built the Q-Q plot: a statistical tool that allows to compare the shapes of two probability distributions by plotting their quantiles alongside. These plots, shown in Fig. 7, support the above argument. Clearly, for both the doorjamb and the wall, the pressure distributions obtained for NO/HC when $\Delta t \leqslant 1$ and $\Delta t > 1$ are identical as the Q-Q plot falls on top of the $x = y$ line. However, when there is an obstacle in front of the door, the quantiles for the distribution corresponding to $\Delta t > 1$ are clearly above the ones belonging to the distribution for $\Delta t \leqslant 1$. This reflects the higher pressures developed at the door when the flow is arrested. As previously discussed, the effect is more important (the distance to the $x = y$ line is greater) when the obstacle is at 50 cm from the door than when it is further away. Also, the differences among the distribution shapes become clearer when considering the doorjamb than the adjacent wall.

5. Conclusions

In this work, we have described the effects that an obstacle placed in front of the exit causes on the local density, velocity, evacuation time and pressure at the door. We have corroborated that if people push each other the result is a reduction of the evacuation time that affects the whole room, and specially the region adjacent to the wall. In these conditions, the placement of the obstacle slightly favours the evacuation of people near the wall, but at the price of considerably increasing the evacuation time of people staying behind the obstacle. These conclusions are in agreement with the overall features of the velocity field, which show two regions between the obstacle and the wall where the velocity is larger. The density maps also reveal the importance of competitiveness and the presence of the obstacle on determining the shape of the field. Interestingly, the density magnitudes observed when pushing was allowed are remarkably higher than in any previous experiment we are aware of.

Concerning the pressure measurements, we have observed a significant increase of the values registered in the highly competitive evacuations. Also, in this scenario, a decreasing trend of the pressure along time is evidenced, probably related to the reduction of people in the room. In addition, for evacuations without obstacle, we have unexpectedly found that there is not any relationship between the pressure and the flowing condition (*i. e.* if the outflow is arrested or not) which is analyzed in terms of the clogging times. The reason for this remains elusive, but the fact that such correlation appears when the obstacle is placed in front of the door prompts us to put forward the following hypothesis. When there is not any obstacle, competitive behavior causes the emergence of high pressures inside the crowd. We speculate that the system is extremely compressed, so the exit of a single pedestrian will not able to relieve the pressure endured by the whole crowd. By placing the obstacle, however, the pressure at the door will be alleviated, but not in the same way for all the flowing conditions. When there is a clog, the pressure is still high (it has almost the same value than for the scenario without an obstacle); but when pedestrians escape from the room, the obstacle would prevent the quick replacement of the empty spaces created, so pressure at the door is reduced. This hypothesis, and other questions still lingering, must be tested in new experiments, that could also address other conditions, including obstacles placed asymmetrically with respect to the exit and mobile obstacles as suggested in Albi et al. (2016).

Acknowledgments

This work was funded by Ministerio de Economía y Competitividad (Spanish Government) through Projects No. FIS2014-57325 and FIS2017-84631-P, MINECO/AEI/FEDER, UE. I.E. acknowledges Asociación de Amigos de la Universidad de Navarra for his grant. We thank L. F. Urrea and J. C. Sánchez for technical help. We are of course indebted to the officers and soldiers of the América 66 Regiment of the Spanish Army who participated in the evacuation drills.

Appendix A. Supplementary material

Supplementary data associated with this article can be found, in the online version, at https://doi.org/10.1016/j.ssci.2019.09.014.

References

Albi, G., Bongini, M., Cristiani, E., Kalise, D., 2016. Invisible control of self-organizing agents leaving unknown environments. SIAM J. Appl. Math. 76 (4), 1683–1710. https://doi.org/10.1137/15M1017016.

Bottinelli, A., Sumpter, D.T.J., Silverberg, J.L., 2016. Emergent structural mechanisms for high-density collective motion inspired by human crowds. Phys. Rev. Lett. 117, 228301. https://doi.org/10.1103/PhysRevLett. 117.228301. URL. <https://link.aps.org/doi/10.1103/PhysRevLett.117.228301>.

Cristiani, E., Peri, D., 2017. Handling obstacles in pedestrian simulations: Models and optimization. Appl. Math. Model. 45, 285–302. https://doi.org/10.1016/j.apm.2016.12.020.. <http://www.sciencedirect.com/science/article/pii/S0307904X16306734>.

Feliciani, C., Nishinari, K., 2018. Measurement of congestion and intrinsic risk in pedestrian crowds. Transport. Res. Part C: Emerg. Technol. 91, 124–155. https://doi.org/10.1016/j.trc.2018.03.027. URL. <http://www.sciencedirect.com/science/article/pii/S0968090X18304133>.

Frank, G., Dorso, C., 2011. Room evacuation in the presence of an obstacle. Physica A 390 (11), 2135–2145. https://doi.org/10.1016/j.physa.2011.01.015. URL. <http://www.sciencedirect.com/science/article/pii/S0378437111000793>.

Garcimartín, A., Zuriguel, I., Pastor, J., Martín-Gómez, C., Parisi, D., 2014. Experimental evidence of the faster is slower effect. Transport. Res. Procedia 2, 760–767, the Conference on Pedestrian and Evacuation Dynamics 2014 (PED 2014), 22–24 October 2014, Delft, The Netherlands. https://doi.org/10.1016/j.trpro.2014.09.085. URL: <http://www.sciencedirect.com/science/article/pii/S2352146514001215>.

Garcimartín, A., Parisi, D.R., Pastor, J.M., Martín-Gómez, C., Zuriguel, I., 2016. Flow of pedestrians through narrow doors with different competitiveness. J. Stat. Mech:

Theory Exp. 2016 (4), 043402. https://doi.org/10.1088/1742-5468/2016/04/043402.
Garcimartín, A., Pastor, J.M., Martín-Gómez, C., Parisi, D.R., Zuriguel, I., 2017. Pedestrian collective motion in competitive room evacuation. Sci. Rep. 7 (1), 10792. https://doi.org/10.1038/s41598-017-11197-x.
Garcimartín, A., Maza, D., Pastor, J.M., Parisi, D.R., Martín-Gómez, C., Zuriguel, I., 2018. New J. Phys. 20 (12), 123025. https://doi.org/10.1088/1367-2630/aaf4ca.
Goldhirsch, I., 2010. Stress, stress asymmetry and couple stress: from discrete particles to continuous fields. Granular Matter 12 (3), 239–252. https://doi.org/10.1007/s10035-010-0181-z.
Haghani, M., Sarvi, M., Shahhoseini, Z., 2019. When push does not come to shove: Revisiting faster is slower in collective egress of human crowds. Transport. Res. Part A: Policy Practice 122, 51–69. https://doi.org/10.1016/j.tra.2019.02.007. URL. <http://www.sciencedirect.com/science/article/pii/S096585641831111X>.
Helbing, D., Farkas, I., Vicsek, T., 2000. Simulating dynamical features of escape panic. Nature 407, 487. https://doi.org/10.1038/35035023.
Helbing, D., Buzna, L., Johansson, A., Werner, T., 2005. Self-organized pedestrian crowd dynamics: Experiments, simulations, and design solutions. Transport. Sci. 39 (1), 1–24. https://doi.org/10.1287/trsc.1040.0108. URL. <https://pubsonline.informs.org/doi/pdf/10.1287/trsc.1040.0108>.
Helbing, D., Johansson, A., Al-Abideen, H.Z., 2007. Dynamics of crowd disasters: An empirical study. Phys. Rev. E 75, 046109. https://doi.org/10.1103/PhysRevE.75.046109. URL. <https://link.aps.org/doi/10.1103/PhysRevE.75.046109>.
Jiang, L., Li, J., Shen, C., Yang, S., Han, Z., 2014. Obstacle optimization for panic flow - reducing the tangential momentum increases the escape speed. PLOS One 9 (12), 1–15. https://doi.org/10.1371/journal.pone.0115463.
Li, L., Liu, H., Han, Y., 2019. Arch formation-based congestion alleviation for crowd evacuation. Transport. Res. Part C: Emerg. Technol. 100, 88–106. https://doi.org/10.1016/j.trc.2019.01.015. URL. <http://www.sciencedirect.com/science/article/pii/S0968090X18309100>.
Lin, P., Gao, D.L., Wang, G.Y., Wu, F.Y., Ma, J., Si, Y.L., Ran, T., 2019. The impact of an obstacle on competitive evacuation through a bottleneck. Fire Technol. https://doi.org/10.1007/s10694-019-00838-4.
Matsuoka, T., Tomoeda, A., Iwamoto, M., Suzuno, K., Ueyama, D., 2015. Effects of an obstacle position for pedestrian evacuation: Sf model approach. In: Chraibi, M., Boltes, M., Schadschneider, A., Seyfried, A. (Eds.), Traffic and Granular Flow '13. Springer International Publishing, Cham, pp. 163–170.
Moussaïd, M., Helbing, D., Theraulaz, G., 2011. How simple rules determine pedestrian behavior and crowd disasters. Proc. Nat. Acad. Sci. 108(17), 6884–6888. arXiv:https://www.pnas.org/content/108/17/6884.full.pdf, https://doi.org/10.1073/pnas.1016507108. URL: <https://www.pnas.org/content/108/17/6884>.
Nicolas, A., Bouzat, S., Kuperman, M.N., 2017. Pedestrian flows through a narrow doorway: Effect of individual behaviours on the global flow and microscopic dynamics. Transport. Res. Part B: Methodol. 99, 30–43. https://doi.org/10.1016/j.trb.2017.01.008. URL. <http://www.sciencedirect.com/science/article/pii/S0191261516307548>.
Pastor, J.M., Garcimartín, A., Gago, P.A., Peralta, J.P., Martín-Gómez, C., Ferrer, L.M., Maza, D., Parisi, D.R., Pugnaloni, L.A., Zuriguel, I., 2015. Experimental proof of faster-is-slower in systems of frictional particles flowing through constrictions. Phys. Rev. E 92, 062817. https://doi.org/10.1103/PhysRevE.92.062817. URL. <https://link.aps.org/doi/10.1103/PhysRevE.92.062817>.
Shi, X., Ye, Z., Shiwakoti, N., Tang, D., Lin, J., 2019. Examining effect of architectural adjustment on pedestrian crowd flow at bottleneck. Physica A 522, 350–364. https://doi.org/10.1016/j.physa.2019.01.086. URL. <http://www.sciencedirect.com/science/article/pii/S0378437119300846>.
Shiwakoti, N., Shi, X., Ye, Z., 2019. A review on the performance of an obstacle near an exit on pedestrian crowd evacuation. Saf. Sci. 113, 54–67. https://doi.org/10.1016/j.ssci.2018.11.016. URL. <http://www.sciencedirect.com/science/article/pii/S0925753518300675>.
Yanagisawa, D., Kimura, A., Tomoeda, A., Nishi, R., Suma, Y., Ohtsuka, K., Nishinari, K., 2009. Introduction of frictional and turning function for pedestrian outflow with an obstacle. Phys. Rev. E 80, 036110. https://doi.org/10.1103/PhysRevE.80.036110. URL: <https://link.aps.org/doi/10.1103/PhysRevE.80.036110>.
Yano, R., 2018. Effect of form of obstacle on speed of crowd evacuation. Phys. Rev. E 97, 032319. https://doi.org/10.1103/PhysRevE.97.032319. URL. <https://link.aps.org/doi/10.1103/PhysRevE.97.032319>.
Yu, W., Johansson, A., 2007. Modeling crowd turbulence by many-particle simulations. Phys. Rev. E 76, 046105. https://doi.org/10.1103/PhysRevE.76.046105. URL. <https://link.aps.org/doi/10.1103/PhysRevE.76.046105>.
Wu, F.Y., Wang, G.Y., Si, Y.L., Lin, P., 2018. An experimental study on the exit location on the evacuation efficiency under high competition condition. Procedia Eng. 211, 801–809. https://doi.org/10.1016/j.proeng.2017.12.078. 2017 8th International Conference on Fire Science and Fire Protection Engineering (ICFSFPE 2017).
Wang, G.Y., Wu, F.Y., Si, Y.L., Zeng, Q., Lin, P., 2018. The study of the impact of obstacle on the efficiency of evacuation under different competitive conditions. Procedia Eng. 211, 699–708. https://doi.org/10.1016/j.proeng.2017.12.066. 2017 8th International Conference on Fire Science and Fire Protection Engineering (ICFSFPE 2017).
Zuriguel, I., Olivares, J., Pastor, J.M., Martín-Gómez, C., Ferrer, L.M., Ramos, J.J., Garcimartín, A., 2016. Effect of obstacle position in the flow of sheep through a narrow door. Phys. Rev. E 94, 032302. https://doi.org/10.1103/PhysRevE.94.032302. URL. <https://link.aps.org/doi/10.1103/PhysRevE.94.032302>.